ELSEVIER

Polymer 41 (2000) 2883–2891

polymer

Light scattering studies on core–shell systems: determination of size parameters of sterically stabilized poly(methylmethacrylate) dispersions

B. Hirzinger[a,*], M. Helmstedt[a], J. Stejskal[b]

[a]*Fakultät für Physik und Geowissenschaften, Abteilung Polymerphysik, Universität Leipzig, Linnéstraße 5, D-04103 Leipzig, Germany*
[b]*Institute of Macromolecular Chemistry, Academy of Sciences of the Czech Republic, Heyrovsky Sq., 16206 Prague 6, Czech Republic*

Received 1 June 1999; received in revised form 30 June 1999; accepted 7 July 1999

Abstract

Poly(methylmethacrylate) dispersions with a weight fraction of the stabilizing diblock copolymer polystyrene-*block*-poly(ethylene-*co*-propylene) $x_S = 0.035$–0.9 and a micellar solution of the diblock copolymer were investigated by static and dynamic light scattering. For high x_S, the R_g/R_h ratio is significantly lower than the value of 0.775 for hard spheres, because of the core–shell structure and different refractive index increments d*n*/d*c* of the polymer components. The core radius R_{core} decreases with increasing stabilizer content, corresponding to a wide range of molar masses. The hydrodynamic shell thickness δ varies only slightly in accordance with previous model calculations whereas the average segment concentration of the stabilizer chains $\langle c_{shell} \rangle$ is practically constant. The number of stabilizing chains per unit surface of the particle core σ_S increases with the shell-to-core mass ratio x_{shell}/x_{core}. During polymerization one dispersion particle grows from one micelle at $x_{shell}/x_{core} \geq 0.25$ while at lower x_{shell}/x_{core} a smaller number of particles with a higher number of block copolymer chains are formed.

Keywords: Light scattering; Core–shell systems; Polymer dispersions

1. Introduction

In sterically stabilized polymer dispersions the polymeric particle core (or body), which is normally insoluble in the surrounding medium, is protected against precipitation by a second polymeric system (the shell or corona) attached to the surface. The stabilizing effect is caused by repulsive forces between the penetrating shells. A wide field of research is occupied with studies on structure and interaction of these systems. The stabilization of dispersion particles by block copolymers has been recently reviewed by Baines et al. [1]. The *quantification* of the forces which are basic for the steric stabilization is of particular interest. Methods like scanning electron microscopy or the recent atomic force microscopy [2] allow only a coarse estimation of size and shape of the particles because the preparation process may be partly modifying or destructive for 'soft' systems and does not allow to observe the particles under natural condition while scattering methods are generally more appropriate for the characterization of dispersed polymer systems.

Small angle X-ray scattering (SAXS) [3] and small-angle neutron scattering (SANS) [4] are well-established methods which can resolve structures of a few nanometers, but especially the latter requires a highly sophisticated apparatus and the usage of partly deuterated samples for contrast enhancement.

Combined static and dynamic light scattering is easy to handle and allows the observation of dispersed systems for the determination of structure *and* interaction parameters by the same set-up. In recent years the determination of various size parameters of core–shell systems by this method has been introduced [5,6].

In our work we consider spherical particles with a solid polymer core of poly(methylmethacrylate) (PMMA), insoluble in the medium *n*-decane, and a stabilizing shell of a soluble polymer with comparatively low segment concentration, which prevents the core from precipitation. In the present system, a diblock copolymer polystyrene-*block*-poly(ethylene-*co*-propylene) (PS–PEP) is used for stabilization, where the aliphatic component (PEP) works as the shell, for which *n*-decane is a good solvent [7]. The micelle formation of this copolymer in *n*-decane and other solvents has previously been studied [8,9]. The aromatic component (PS) is entangled with the PMMA core during the polymerization process and serves as the so-called anchor, although PMMA and PS are incompatible with respect to binary

* Corresponding author. Tel.: +49-341-97-32572; fax: +49-341-97-32497.

0032-3861/00/$ - see front matter
PII: S0032-3861(99)00472-3

Table 1
PMMA dispersions and their size parameters: x_S is the weight fraction of the stabilizing diblock copolymer Kraton® and c_0 the total particle concentration after polymerization; M_w is the weight-average particle molar mass and M_w/M_n the weight-to-number average molar mass ratio, showing the polydispersity; R_g and R_h are the radius of gyration and the hydrodynamic radius, respectively

Sample	x_S	c_0 (g cm^{-3})	$M_w \times 10^{-6}$ (g mol^{-1})	M_w/M_n	R_g (nm)	R_h (nm)	R_g/R_h
D5	0.0351	0.143	4240	1.61	110	135	0.814
D10	0.0517	0.194	9730	1.33	141	175	0.806
D6	0.0678	0.148	1270	1.29	69.1	113	0.614
D7	0.0983	0.153	552	1.46	58.5	89.4	0.654
D8	0.127	0.158	402	1.88	52.7	80.6	0.653
D3	0.146	0.103	124	1.28	42.9	61.4	0.699
D4	0.185	0.108	92.6	1.35	43.3	57.3	0.755
X2	0.199	0.0503	68.4	1.28	46.0	61.6	0.746
P1	0.200	0.0933	39.2	1.31	33.9	60.3	0.562
X3	0.272	0.0553	64.2	1.39	33.0	57.3	0.576
Z1	0.300	0.0300	17.3	1.08	22.3	49.3	0.453
P2	0.400	0.0486	14.6	1.18	25.4	50.8	0.500
Z2	0.400	0.0300	12.5	1.09	22.0	48.4	0.454
Z3	0.500	0.0300	13.2	1.13	26.7	48.1	0.555
P3	0.600	0.0329	9.03	1.27	26.1	46.7	0.559
Z4	0.600	0.0300	9.08	1.14	23.3	46.8	0.499
Z5	0.700	0.0300	8.64	1.19	26.6	48.5	0.549
Z6	0.800	0.0300	7.42	1.16	25.6	48.5	0.527
P4	0.800	0.0249	6.81	1.18	24.4	44.9	0.543
Z7	0.900	0.0300	7.02	1.22	26.1	48.5	0.537
Kraton®	1.000	0.0200	4.92	1.08	23.1	42.2	0.548

blends. However, these two polymers have similar densities [10], are both insoluble in *n*-decane and are in the glassy state at $T \leq 100$°C [11], so one can regard them simplified as one system denoted as 'core'.

The aim of this paper is to show the dependence of the particle structure on the relative amount of the stabilizing polymer over a wider range than described in previous works. Further, conclusions to the particle formation during the process of polymerization will be made.

2. Experimental

2.1. Polymerization

A micellar solution of the stabilizing diblock copolymer (polystyrene-*block*-(ethylene-*co*-propylene); Kraton® G 1701, Shell Co.; 34 wt.% of polystyrene, $M_w^S = 1.05 \times 10^{-5}$ g mol^{-1}, $M_w/M_n = 1.24$ [8]) was prepared in *n*-decane (Fluka, Switzerland). The solution was heated to 70°C for 4 h and cooled down again to room temperature to obtain a solution of 'frozen' micelles [8,9] in a stable state with no exchange of unimers. Subsequent filtration through a 0.8 μm membrane filter (Millipore) was performed to remove insoluble impurities. Then a specified amount of the initiator, azo-isobutyronitrile (AIBN; Fluka), dissolved in methylmethacrylate (MMA; Lachema, Czech Republic, purified in laboratory) was added to the solution. The concentration of the initiator was kept constant at 1.0×10^{-3} g cm^{-3} while the mass fraction of the stabilizer has been varied widely. The mixtures were sealed in glass ampoules and were heated, for polymerization, to 60°C for 70 h. After polymerization no free stabilizer was left behind [5]. Under these conditions, dispersion particles with PMMA/PS core and PEP shell are produced.

In the first instance, samples denoted X1–X4 and D1–D15 with relatively low weight fractions of the steric stabilizer had been polymerized and the particle characteristics have been already published [5,13]. For the present study, additional sets of samples Z1–Z7 and P1–P4 with higher weight fractions of the steric stabilizer, x_S, have been prepared. A subset of the samples X1–D15 was still available and has been taken into this study again due to improvements in the apparatus set-up and data analysis, as described below. For comparison with the dispersions, a micellar solution the block copolymer, 'Kraton®', has been used.

For the samples Z1–Z7 and P1–P4, 100% conversion of monomer to polymer is assumed, since weighing of the remaining solid polymer after drying did not reveal significantly lower values like the previous studies on the dispersions X1–D15 [6]. The mass fraction of the stabilizer x_S and the total particle concentration c_0 of PMMA and PS–PEP after polymerization are given in Table 1.

2.2. Determination of particle parameters by light scattering

On the dispersions X2, X3, D3–D8, D10, Z1–Z7, P1–P4 and the micellar Kraton® solution both static and dynamic light scattering were carried out at $T = (25.00 \pm 0.01)$°C by a DLS–SLS 5000 Laser Light Scattering Goniometer

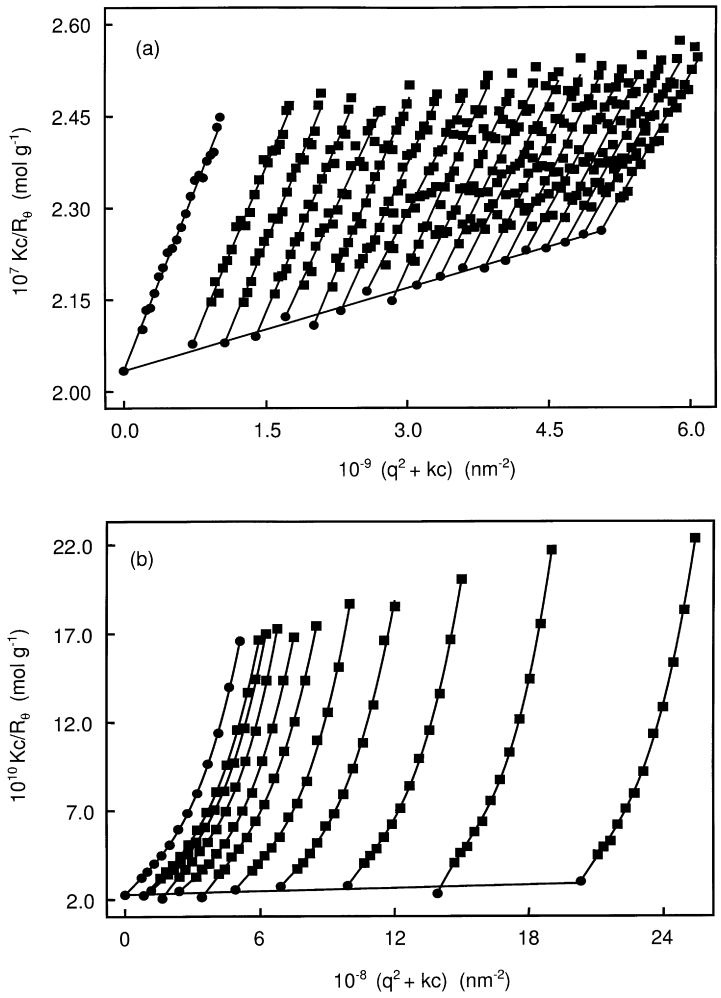

Fig. 1. Zimm plot of (a) micellar solution of the stabilizer Kraton® and (b) of the PMMA-dispersion D5 (weight fraction of stabilizer $x_S = 0.0351$) in *n*-decane.

(ALV; Langen, Germany), equipped with a 140 mW Nd:YAG laser (diode pumped, frequency doubled, wavelength $\lambda_0 = 532$ nm; ADLAS, Lübeck, Germany) and a ALV-5000 Multiple Tau digital correlator. The measured data were directly recorded by a personal computer.

Dynamic light scattering (DLS) measurements were performed at appropriate dilution at angles $\theta = 30$, 45, 60, 90 and 120°. At $\lambda_0 = 532$ nm and $T = 25$°C, the refractive index of the solvent *n*-decane is $n = 1.4125$. In expressions concerning light scattering, usually it is not the scattering angle θ that is directly used, but the scattering vector **q**, with

$$q = \frac{4\pi n}{\lambda_0} \sin \frac{\theta}{2}. \quad (1)$$

The measured intensity autocorrelation functions $g_2(t)$ were fitted to the Pearson distribution as described in Ref. [6], using the General Exponential (GEX) method from the program GENDIST [14], giving more reliable results than the CONTIN inversion method [15,16], in our case. Two parameters were varied during the fitting process: the relaxation time τ_{GEX}, being the peak position of the fitted distribution function, and the dimensionless parameter *p*, where a large *p* value corresponds to a small peak width. The obtained translational diffusion coefficients, given by $D_t = 1/(q^2 \tau_{GEX})$, were practically independent of concentration for dilutions higher than 1:25. The hydrodynamic radii R_h (Table 1) were calculated from zero angle limits of diffusion coefficients by the Stokes–Einstein equation

$$D_t = \frac{kT}{6\pi \eta_0 R_h} \quad (2)$$

where k is the Boltzmann constant and η_0 the viscosity of the ambient solvent. The dependence $R \sim M^{1/3}$ for hard spheres was assumed, referring to the distribution of radius and molar mass, respectively, within one sample. Therefore, the weight-to-number average molar mass ratio M_w/M_n (Table 1), which expresses the polydispersity, can be calculated by

$$M_w/M_n = (p + 5)(p + 4)(p + 3)/[(p + 2)(p + 1)p].$$

At static light scattering (SLS), the inverse reduced scattering intensity Kc/R_θ and its dependence on the scattering

angle θ provide the weight-average molar mass M_w of the dispersion particles and the particle size, described by the *z*-average radius of gyration $R_g \equiv \langle s^2 \rangle_z^{1/2}$, according to the Rayleigh–Debye approximation

$$\frac{Kc}{R_\theta} = \frac{1}{P(\theta)}\left(\frac{1}{M_w} + 2A_2c + \cdots\right), \quad K = \frac{4\pi n^2 (dn/dc)^2}{N_A \lambda_0^4} \tag{3}$$

with K being the contrast factor for vertically polarized light of wavelength λ_0 in vacuo, c the mass concentration of the dispersion, $R_\theta \equiv r^2(I_\theta/I_0)$ the Rayleigh ratio, I_θ and I_0 the intensities at the distance r and at angle of observation θ and 0°, respectively. The form factor $P(\theta)$ generally depends on particle size and shape, giving the angle dependence of the scattering intensity, while A_2, the second virial coefficient, is provided by the concentration dependence. n is the refractive index of the dispersion medium, dn/dc the refractive index increment of the polymer system and N_A the Avogadro number.

For the SLS measurements in the present work, all samples mentioned above were highly diluted in *n*-decane. The maximum concentration of one series of dilution varied from 1×10^{-5} to 5×10^{-4} g cm^{-3}. The range for the scattering angles was either $\theta = 15, \ldots, 90°$ or $\theta = 30, \ldots, 150°$, with steps of 5°. Since the refractive index increments dn/dc of PMMA and PS–PEP are known (0.082 and 0.121 cm^3 g^{-1}, respectively, for $\lambda_0 = 532$ nm), the resulting dn/dc value has been calculated for each sample [5].

The common method of analysis for SLS data is the Zimm plot, where the form factor is given by

$$P(\theta) \approx 1 - \frac{1}{3}q^2 R_g^2, \tag{4}$$

independent of the particle geometry. This approximation can be applied relatively successful for $q^2R_g^2 < 1$ and low M_w/M_n, even for wider angles θ. Then Kc/R_θ can be fitted linearly versus q^2, which is the case for the micellar Kraton® solution, as shown in Fig. 1a, and similarly for all PMMA dispersions with $x_S \geq 0.3$, corresponding to particles with $R_g < 30$ nm. For dispersions with $x_S \leq 0.3$, the dependence of Kc/R_θ on q^2 is not linear any more due to higher radii of gyration $R_g > 30$ nm (see Fig. 1b). In practice, the shown polynomial fit of Kc/R_θ versus q^2 is not sufficiently precise. Also, the effect of polydispersity becomes stronger with increasing particle size. Because of the low mass fraction x_{PEP} of the shell, the larger PMMA particles can be regarded as hard spheres and $P(\theta)$ can be described by the Rayleigh hard sphere model. This model was extended for a log–normal molar mass distribution with polydispersity M_w/M_n, as described by Francuskiewicz and Dauzenberg [17]:

$$P(\theta) = \frac{1}{M_w}\int_0^\infty M\, p_w(M) P_M(\theta)\, dM,$$
$$M_w \equiv \int_0^\infty M\, p_w(M)\, dM \tag{5}$$

with

$$p_w(M) = \frac{M^{-3/2}\exp(-(\ln M - \ln M_w)^2/2\sigma^2)}{(2\pi)^{1/2}\sigma M_w^{-1/2}\exp(\sigma^2/8)},$$
$$M_w/M_n = \exp(\sigma^2) \tag{6}$$

and

$$P_M(\theta) = \left(3\frac{\sin X - X\cos X}{X^3}\right)^2,$$
$$X = \left(\frac{5}{3}\right)^{1/2} qR_g\left(\frac{M}{M_w}\right)^{1/3}\exp\left(-\frac{5}{18}\sigma^2\right). \tag{7}$$

For each concentration c of a series, the static light scattering data Kc/R_θ vs q^2 was least-square fitted with the parameters M_w and R_g while the M_w/M_n value obtained previously from DLS data analysis was kept constant. For more reliable results, a self-developed PC program was used for fitting, which allows visual pre-adjusting of the fit parameters before running of the automatic fit routine. $1/M_w(c)$ and $R_g^2(c)$ were then linearly extrapolated to $c = 0$ to obtain the values of M_w and R_g which are given in Table 1.

For small particles with high x_S, we also have applied the hard sphere model, as a compromise. A special model for core–shell particles would have to take the different refractive index increments dn/dc of core and shell into account. This would not be in accordance with the Rayleigh–Debye approximation, which implies the separation of optical and geometrical scattering parameters. Due to the consideration of the polydispersity, the extended hard sphere model has still an advantage over the straightforward Zimm plot and delivers radii of gyration R_g which are about 5% lower, while the molar masses M_w obtained from both models are practically identical. Since $q^2R_g^2 < 1$ and $P(\theta)$ can be approximated by Eq. (4), a core–shell model would not reveal significantly different values of the radius of gyration R_g. However, R_g requires further interpretation, as discussed in the next section.

Additional size parameters are derivable from M_w, R_g and R_h, according to Refs. [6,13], like the core radius

$$R_{core} = \left(\frac{3M_n^D}{4\pi N_A}\left(\frac{x_{PMMA}}{\rho_{PMMA}} + \frac{x_{PS}}{\rho_{PS}}\right)\right)^{1/3}, \tag{8}$$

the hydrodynamic shell thickness

$$\delta = R_h - R_{core}, \tag{9}$$

the average segment concentration of stabilizer chains

$$\langle c_{shell}\rangle = \frac{3}{4\pi N_A}\frac{x_{PEP}M_n^D}{(R_h^3 - R_{core}^3)} \tag{10}$$

as well as the number density of stabilizing shell chains per surface unit of the particle core

$$\sigma_S = \frac{1}{4\pi R_{core}^2}\frac{M_n^S}{x_S M_n^D}, \tag{11}$$

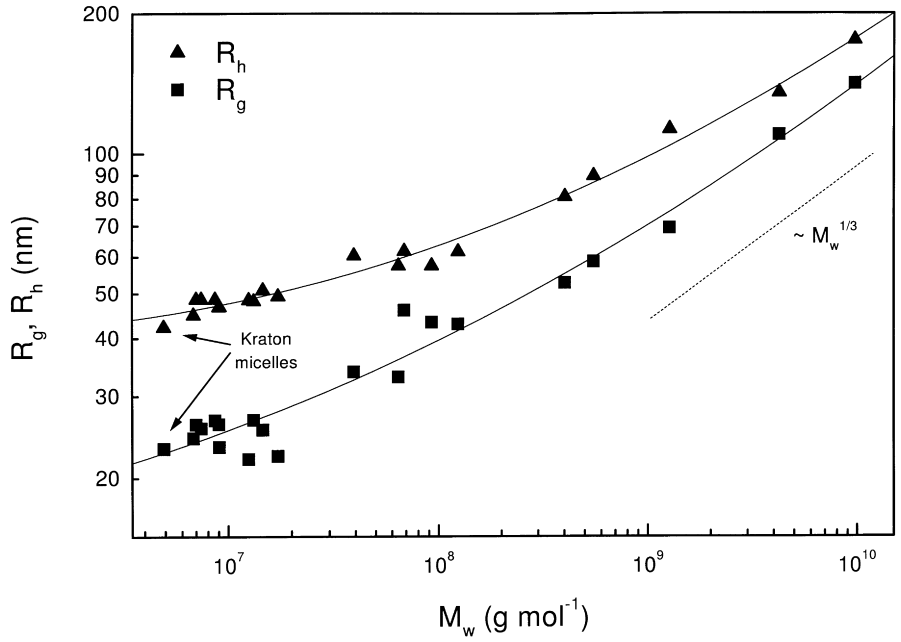

Fig. 2. Relation of the radius of gyration R_g and the hydrodynamic radius R_h to the weight average particle molar mass M_w.

with $\rho_{PMMA} = 1.17$ g cm^{-3} and $\rho_{PS} = 1.05$ g cm^{-3} being the solid state polymer densities [10], $x_{PMMA} = 1 - x_S$, $x_{PS} = 0.34x_S$ and $x_{PEP} = 0.66x_S$ the weight fractions of the polymer components and M_n^D and M_n^S the number-average molar mass of the dispersion particle and a single chain of the stabilizer, respectively. Particularly the parameters $\langle c_{shell} \rangle$ and σ_S are useful in description of the stability of the dispersion particles.

3. Results and discussion

3.1. Basic size parameters

The weight-average molar mass M_w of the dispersion particles decreases strongly with increasing mass fraction of the stabilizer x_S over three orders of magnitude (Table 1). Also, a weaker tendency can be seen, that a larger absolute concentration of MMA plus stabilizer leads to the formation of larger particles. The radius of gyration behaves analogously at low x_S but asymptotically reaches a value of about 23 nm at high x_S. In the former case the weight of the particle is dominated by the compact core, in the latter case the dimensions are controlled mainly by the shell. The hydrodynamic radii behave similar with a value of about 42 nm at high x_S. The table also contains the size parameters of the *micellar* Kraton® solution which match the behaviour of the dispersions well.

The dependence of the particle radii R_h and R_g on M_w is shown in Fig. 2. For hard spheres, R_h and R_g are expected to be proportional to $M^{1/3}$. With increasing stabilizer fraction x_S and decreasing molar mass M_w, the dispersion particles deviate more and more from this behaviour. As discussed in detail in the next subsection concerning additional size parameters, mainly the core radius R_{core} changes significantly with the molar mass M_w while the shell thickness δ stays relatively constant. It is obvious that for small particles with low M_w and $R_{core} < \delta$, the change of $R_h = R_{core} + \delta$ with M_w is much smaller than for large particles with high M_w and $R_{core} > \delta$. Hence, a power law $R_g \sim R_h \sim M^a$ cannot be applied for the present range of molar masses. The slope $a = d(\ln R_h)/d(\ln M_w)$ is much smaller than 1/3 for particles with low M_w. Plotting R_g versus M_w shows a similar behaviour because R_g and R_h are in the same order of magnitude. Since the ratio R_g/R_h increases slightly with M_w, as discussed in the following paragraph, $a' = d(\ln R_g)/d(\ln M_w) > a$ is found for the whole range of molar masses M_w of this study. At the highest molar mass of the series of samples, $M_w = 9.73 \times 10^9$ g mol^{-1}, the slopes have reached values of $a = 0.288$ for $R_h(M_w)$ and $a' = 0.329$ for $R_g(M_w)$, respectively.

In the limit of zero weight fraction of stabilizer x_S, the R_g/R_h relation (Table 1) approaches the value $(3/5)^{1/2} \approx 0.775$ for hard spheres, as described in Ref. [13]. At high x_S, R_g/R_h approximates a value of 0.5. $R_g/R_h < 0.775$ is not expected for dissolved macromolecules. On microgels of poly(butylmethacrylate) similar results were obtained by Kunz et al. [18]. In our work, this extraordinary behaviour of the dispersion particles can be explained as follows:

As mentioned in the discussion of additional size parameters in the next subsection, the average segment concentration $\langle c_{shell} \rangle$ in the soft PEP shell of a dispersion particle is about 1.5% of the solid state density, $\rho_{PEP} = 0.85$ g cm^{-3} [11], but still higher than in a gaussian coil of comparable size. Therefore, the solvent molecules within the shell are immobilized and the hydrodynamic radius R_h

Table 2
Additional size parameters of the PMMA dispersions: x_{shell}/x_{core} is the shell-to-core mass ratio; R_{core} and δ are the particle core radius and the hydrodynamic shell thickness; $\langle c_{shell}\rangle$ and σ_S, respectively, are the average segment concentration of the stabilizer chains and the number of chains per unit surface of the core; N_D/N_M is the ratio of the number of dispersion particles after polymerization to the number of starting Kraton® micelles before the addition of MMA

Sample	x_{shell}/x_{core}	R_{core} (nm)	δ (nm)	$\langle c_{shell}\rangle$ (g cm^{-3})	σ_S (nm^{-2})	N_D/N_M
D5	0.0237	95.6	39.1	0.0154	0.00951	0.0495
D10	0.0353	134	41.1	0.0334	0.0198	0.0121
D6	0.0468	68.3	44.3	0.0157	0.0134	0.0686
D7	0.0694	49.4	40.0	0.0163	0.0143	0.123
D8	0.0914	40.6	40.0	0.0155	0.0155	0.169
D3	0.106	31.0	30.4	0.0183	0.0138	0.325
D4	0.139	27.4	29.9	0.0198	0.0159	0.360
X2	0.151	25.1	36.5	0.0128	0.0158	0.430
P1	0.152	20.7	39.6	0.00746	0.0132	0.763
X3	0.218	23.5	33.8	0.0187	0.0213	0.365
Z1	0.247	16.4	32.9	0.0109	0.0168	0.956
P2	0.359	14.7	36.1	0.0101	0.0216	0.925
Z2	0.359	14.3	34.1	0.0109	0.0211	0.994
Z3	0.493	14.0	34.1	0.0142	0.0282	0.777
P3	0.656	11.5	35.2	0.0111	0.0305	1.073
Z4	0.656	11.9	34.8	0.0125	0.0316	0.956
Z5	0.859	11.2	37.3	0.0119	0.0384	0.896
Z6	1.119	10.3	38.2	0.0118	0.0454	0.895
P4	1.119	9.9	34.9	0.0135	0.0439	0.991
Z7	1.463	9.5	39.0	0.0119	0.0538	0.885
Kraton®	1.941	8.4	33.8	0.0160	0.0613	–

can approximately be regarded as the geometric radius. The radius of gyration R_g, however, is determined by the distribution of the scattering centres in the particle. The particles are optically inhomogeneous, i.e. consist of three polymers PMMA, PS and PEP with different refractive index increments ν_i. For the light scattering measurements, only the average refractive index increment of the particle, $dn/dc = \nu = x_{PMMA}\nu_{PMMA} + x_{PS}\nu_{PS} + x_{PEP}\nu_{PEP}$ is taken into account. At $\lambda_0 = 532$ nm and $T = 25$°C, $\nu_{PMMA} = 0.082$ cm^3 g^{-1}, $\nu_{PS} = 0.178$ cm^3 g^{-1} and $\nu_{PEP} = 0.092$ cm^3 g^{-1} [10–12].

We assume that PMMA and PS mix homogeneously within the compact core and have solid state density. The soft PEP shell can be described as a hollow sphere with a $c_{shell}(r) \sim r^{-4/3}$ segment concentration profile [19], which will be further discussed in the following subsection.

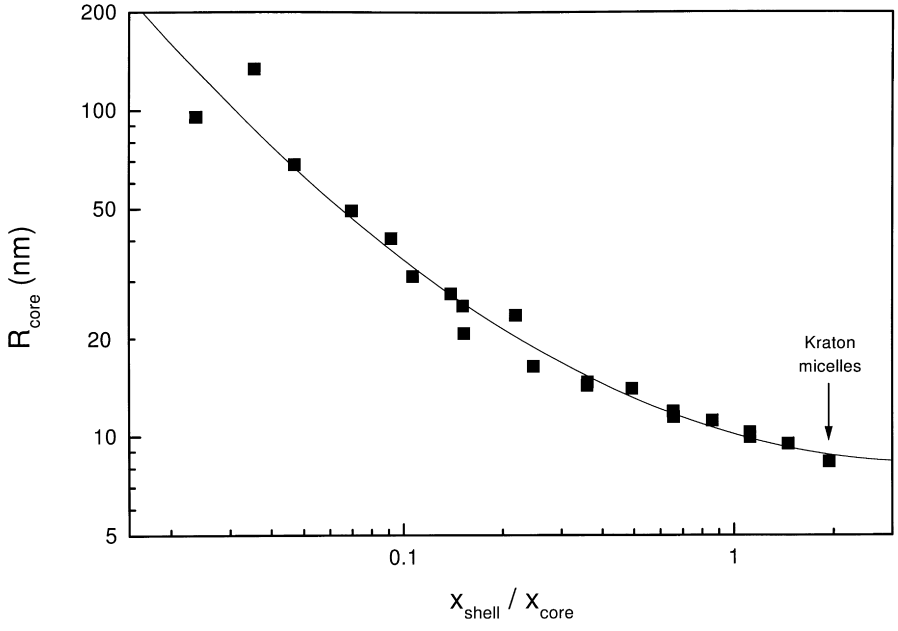

Fig. 3. Dependence of the core radius R_{core} on the shell-to-core mass ratio x_{shell}/x_{core}.

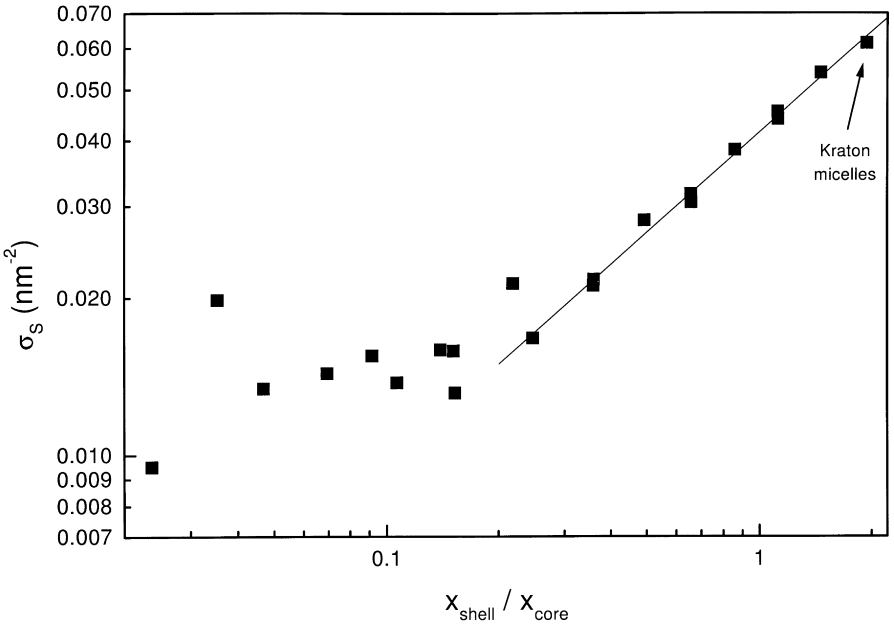

Fig. 4. Variation of the number of stabilizing chains per surface unit of the particle core σ_S versus the shell-to-core mass ratio x_{shell}/x_{core}.

Modifying Eq. (9) from Ref. [5] in this way, an expression for the apparent radius of gyration R_g^{app} can be given as

$$R_g^{app} = \left(\frac{3}{5} \frac{x_{PMMA}\nu_{PMMA} + x_{PS}\nu_{PS}}{\nu} R_{core}^2 + \frac{5}{11} \frac{x_{PEP}\nu_{PEP}}{\nu} \frac{R_h^{11/3} - R_{core}^{11/3}}{R_h^{5/3} - R_{core}^{5/3}} \right)^{1/2}. \quad (12)$$

Due to the high refractive index increment of the PS in the core and the sloping segment concentration profile of the PEP shell, small particles with a high stabilizer fraction x_S have the apparent scattering centre shifted toward the core, compared to a compact homogeneous sphere, and show a $R_g/R_h < 0.775$ relation. Eq. (12) approximates to $R_g^{app}/R_h = [(5/11) \times 0.66 \times 0.092/0.121]^{1/2} \approx 0.476$ for $x_S \rightarrow 1$ and $R_h \gg R_{core}$ while for $x_S \rightarrow 0$ it becomes the relation $R_g^{app}/R_h = (3/5)^{1/2} \approx 0.775$ for hard spheres.

In comparison to the measured R_g values, the calculated R_g^{app} values may be somewhat smaller, particularly for low x_S. Static light scattering has the tendency to overestimate the radius of gyration if a very small fraction of aggregates with high molar mass is present in the dispersion [13]. Also, Eq. (12) does not contain mixing terms, i.e. the interference of light scattered from different polymer components of a particle is not considered.

3.2. Additional size parameters

One can derive some more information from the directly measurable size parameters (Table 2). The shell-to-core ratio $x_{shell}/x_{core} = x_{PEP}/(x_{PMMA} + x_{PS}) = 0.66x_S(1 - 0.66x_S)$ seems to be a more appropriate parameter for data ordering than x_S. The core radius, according to Eq. (8), decreases systematically with increasing value of x_{shell}/x_{core} (Fig. 3), indicating the equilibrium between surface and volume of the liquid MMA during the polymerization process in the presence of the Kraton® micelles.

The hydrodynamic shell thickness δ (Eq. (9)) is not expected to change significantly with the particle size, since the block copolymer micelles swollen with MMA fill with PMMA during polymerization and change to dispersion particles. Indeed, δ varies only between 30 and 40 nm for almost all samples, which is larger than the average end-to-end distance $\langle h^2 \rangle^{1/2} \approx 26$ nm of free PEP chains with corresponding molar mass [6]. We expect that the PEP chains deviate from the coil structure and stretch when they are attached to the surface of the core.

Model calculations for practically identical core–shell systems have been published by Procházka and Stejskal [20]. The correlation between the shell thickness and the Flory–Huggins interaction parameter χ has been calculated. The authors found $\delta = 21$ nm for $\chi = 0.5$. However, our value $\delta \approx 35$ nm agrees well with the δ given for $\chi \approx 0.348$ in Ref. [7].

The average segment concentration of stabilizer chains $\langle c_{shell} \rangle$ (Eq. (10)) is between 0.01 and 0.02 g cm^{-3} for almost all particles and does not relate to their size. However, c_{shell} is expected to decrease with increasing distance r from the centre of the particle. In the dilute region in a good solvent a $c_{shell}(r) \sim r^{-4/3}$ dependence was introduced by Daoud and Cotton [19] more than a decade ago.

The number density of the block copolymer chains per surface unit of the particle core σ_S (Eq. (11)) is approximately

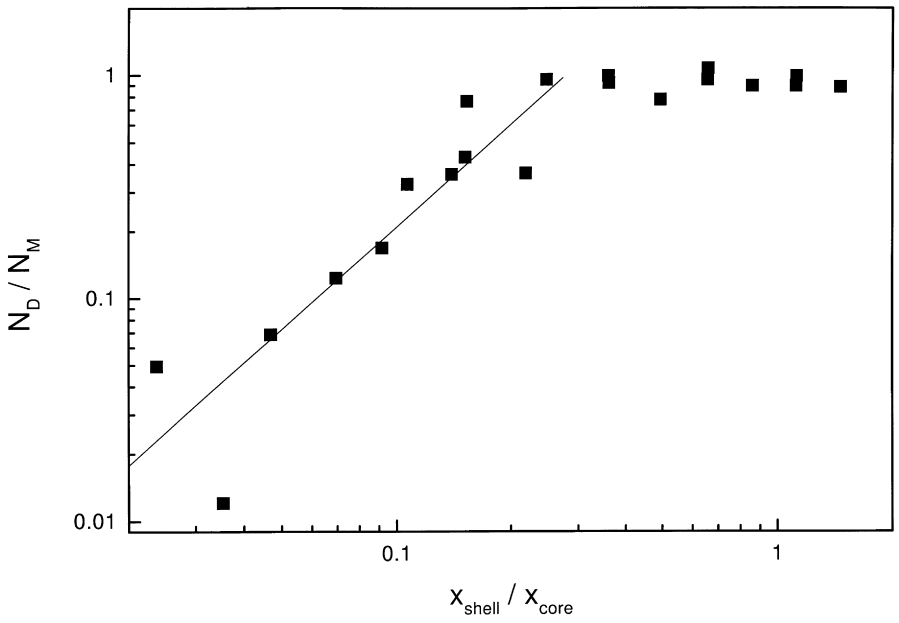

Fig. 5. The number ratio N_D/N_M of dispersion particles after polymerization to Kraton® micelles before addition of MMA versus the shell-to-core mass ratio x_{shell}/x_{core}.

constant, about $0.015\,nm^{-2}$, at $x_{shell}/x_{core} \leq 0.25$ and increases at higher shell-to-core mass ratios with a power law, $\sigma_S \sim (x_{shell}/x_{core})^{0.64}$ (Fig. 4), being one of the main characteristics of the quality of stabilization.

The ratio of the number of dispersion particles after polymerization to the number of starting Kraton® micelles before the addition of MMA,

$$\frac{N_D}{N_M} = \frac{1}{x_S}\frac{M_n^M}{M_n^D}, \tag{13}$$

with M_n^D and M_n^M the number average molar masses of the dispersion particles and the Kraton® micelles, respectively, is of particular interest: Since MMA is a good solvent for PS, the addition of a smaller amount of MMA to the Kraton® micellar solution (corresponding to a higher shell-to-core mass ratio of the dispersion particles $x_{shell}/x_{core} \geq 0.25$) leads to the absorption of MMA in the PS cores with swelling. However, the association number (i.e. the number of the block copolymer chains per micelle) will not change. During the subsequent process of polymerization one dispersion particle approximately will grow from one micelle (Fig. 5). If the amount of the added MMA is higher, the micelles will overcome the frozen state and reorganize to a smaller number of larger units with a higher number of block copolymer chains. The polymerization will again proceed within the (now restructured) micelles. This behaviour expresses in a power dependence, $N_D/N_M \sim (x_{shell}/x_{core})^{1.53}$.

To correlate the second virial coefficient with structural parameters as a measure for the quality of steric stabilization is the aim of the next contribution of this series.

4. Conclusions

Parameters obtainable from the basic results of static and dynamic light scattering on PMMA dispersions in *n*-decane stabilized with polystyrene-*block*-poly(ethylene-*co*-propylene) are helpful in the discussion of the stability of the particles, differing strongly in stabilizer content x_S as in molar mass M_w. The stabilizer content was varied over wider range than in previous studies. Measurements on a micellar solution of the stabilizer were performed for comparison. The particles created for this study fill the gap between 'classical' latex particles and star polymers.

For high x_S, the R_g/R_h ratio reaches values of about 0.5 which is significantly lower than the value of $(3/5)^{1/2} \approx 0.775$ expected for hard spheres. This unconventional behaviour is caused by the core–shell structure and different refractive index increments dn/dc of the polymer components. The core radius R_{core} decreases with increasing stabilizer content, corresponding to a range of molar masses over three and a half orders of magnitude. The hydrodynamic shell thickness δ varies only slightly in accordance with the previous model calculations. While the segment concentration of the stabilizer chains c_{shell} is expected to have a $r^{-4/3}$ dependence, the average value $\langle c_{shell} \rangle$ is practically constant. The number of stabilizing chains per unit surface of the particle core σ_S increases with the shell-to-core mass ratio x_{shell}/x_{core}. Comparing the number of dispersion particles N_D with the number of the stabilizing diblock copolymer micelles N_M before addition of the MMA monomer leads to the conclusion that during polymerization one dispersion particle grows from one micelle at $x_{shell}/x_{core} \geq 0.25$ while at lower shell-to-core mass ratio a smaller number of

particles with a higher number of block copolymer chains is formed.

Acknowledgements

The authors are indebted to the Deutsche Forschungsgemeinschaft for the support by the SFB 294 “Molecules in Interaction with Interfaces”, project B4, and the project He 2123/2-3 (including 436 TSE-113/6). We are also obliged to Dr Č. Koňák, Institute of Macromolecular Chemistry, Prague, for valuable discussions.

References

[1] Baines FL, Dionisio S, Billingham NC, Armes SP. Macromolecules 1996;29:3096.
[2] Lea AS, Andrade JD, Hlady V. Colloids Surf A 1994;93:349.
[3] Dingenouts N, Kim JS, Ballauf M. Macromol Rapid Commun 1994;15:613.
[4] Mills MF, Gilbert RG, Napper DH, Rennie AR, Ottewill RH. Macromolecules 1993;26:3553.
[5] Stejskal J, Kratochvíl P, Koubík P, Tuzar Z, Urban J, Helmstedt M, Jenkins AD. Polymer 1990;31:1816.
[6] Stejskal J, Kratochvíl P, Koňák Č. Polymer 1991;32:2435.
[7] Barton AFM. CRC handbook of polymer–liquid interaction parameters and solubility parameters. Boca Raton, FL: CRC Press, 1990.
[8] Stejskal J, Hlavatá D, Sikora C, Koňák Č, Pleštil J, Kratochvíl P. Polymer 1992;33:3675.
[9] Hlavatá D, Stejskal J, Pleštil J, Koňák Č, Kratochvíl P, Helmstedt M, Mio H, Laggner P. Polymer 1996;37:799.
[10] Van Krevelen DW, Hoftyzer PJ. Properties of polymers, 2nd ed. Amsterdam: Elsevier, 1976.
[11] Brandrup J, Immergut EH, editors. Polymer handbook. New York: Wiley, 1989.
[12] Landolt-Börnstein Zahlenwerte and Funktionen aus Physik, Chemie, Astronomie, Geophysik and Technik, 6 Auflage, II Band, 8 Teil, Optische Konstanten. Berlin/Göttingen/Heidelberg: Springer Verlag, 1962.
[13] Helmstedt M, Schäfer H. Polymer 1994;35:3377.
[14] Johnsen R. GENDIST program description, Uppsala, 1995.
[15] Provencher SW. Comput Phys Commun 1982;27:213.
[16] Provencher SW. Comput Phys Commun 1982;27:229.
[17] Francuskiewicz F, Dautzenberg H. Eur Polym J 1985;21:455.
[18] Kunz D, Thurn A, Burchard W. Colloid Polym Sci 1983;261:635.
[19] Daoud M, Cotton JP. J Phys 1982;43:531.
[20] Procházka O, Stejskal J. Polymer 1992;33:3658.